Effects of Diffusion-Controlled Reactions on Atom-Transfer Radical Polymerization

Omar Delgadillo-Velázquez, Eduardo Vivaldo-Lima, and Iraís A. Quintero-Ortega
Dept. de Ingeniería, Química, Facultad de Química, Universidad Nacional Autónoma de México (UNAM), Conjunto E, Ciudad Universitaria, México D. F., CP 04510, México

Shiping Zhu
Dept. of Chemical Engineering and Dept. of Materials Science and Engineering, McMaster University, Hamilton, Ontario, Canada, L8S 4L7

A kinetic model incorporating effects of diffusion-controlled reactions on atom-transfer radical polymerization (ATRP) was developed. The reactions considered to be diffusion-controlled are monomer propagation, bimolecular radical termination, chain transfer between propagating radical and catalyst, and transfer to small molecules. Model predictions indicate that a diffusion-controlled propagation reduces the "living" behavior of the system, whereas a diffusion-controlled termination enhances its livingness. When diffusion-controlled transfer between chains and catalyst is considered the same in the forward and backward directions, the livingness of the system is enhanced, but if one of them is kept unchanged while the other is increased, the livingness of the system is reduced. When diffusion-controlled termination is important, our simulations show that the overall effect of diffusion-controlled phenomena in ATRP is to enhance the livingness of the system. Experimental data from the literature for styrene, methyl methacrylate, and methyl acrylate ATRP homopolymerizations validate the kinetic model.

Introduction

Controlled-radical polymerization (CRP) has become a major field in polymer science and engineering. CRP is also known as "pseudoliving" radical polymerization. A polymerization process is considered to be living if the growing chains do not experience permanent termination and/or transfer during the course of polymerization. The current most effective and versatile CRP processes are (1) stable free-radical polymerization (SFRP), best represented by nitroxide-mediated polymerization (NMP), (2) metal-catalyzed atom-transfer radical polymerization (ATRP), and (3) reversible addition-fragmentation chain transfer (RAFT) polymerization, along with other degenerative transfer processes. The common feature in these processes is the dynamic equilibration between growing free-radicals and various types of dormant species. The difference among them is due to the mechanism and chemistry of the equilibration/exchange process (Matyjaszewski, 2000). The *ini*tiator-trans*fer* agent-*ter*minator (Iniferter) technique, proposed by Otsu and Yoshida (1982), is also used to promote a "living" character in free-radical polymerization.

While the literature on the chemistry of these processes is extensive (for example, Matyjaszewski, 2000; Colombani, 1997), the kinetic aspects, such as the evaluation of kinetic rate constants and the development of mathematical kinetic models, are less developed. Shi et al. (1999) presented a kinetic model for ideal living radical polymerization, based on the method of moments, which included initiation by thermal dissociation of capped unimers, propagation, and capping/uncapping reactions, thus neglecting bimolecular termination. Zhu (1999a,b) developed kinetic models for ATRP and SFRP based on the method of moments, and presented extensive simulation studies on the effects of the main reagents and kinetic parameters on molecular-weight development. Using the Predici polymerization software of CiT,

Correspondence concerning this article should be addressed to E. Vivaldo-Lima.

Matyjaszewski's group has modeled the polymerization of styrene in the presence of a stable radical, 2,2,6,6-tetramethyl-1-piperidinyloxy (TEMPO), considering thermal initiation, but neglecting diffusion-controlled reactions (Greszta and Matyjaszewski, 1996); the ATRP of styrene, modeling diffusion controlled termination with a semiempirical equation dependent on conversion and number-average chain length (Shipp and Matyjaszewski, 1999), and focusing on the complex kinetics represented by noninteger reaction orders, as well as the effect of heterogeneous polymerization conditions (Shipp and Matyjaszewski, 2000). Butté et al. (2000) developed a kinetic model for NMP-SFRP and ATRP linear styrene homopolymerizations using the method of moments and an empirical expression for diffusion-controlled termination. Fukuda et al. (2000) measured some activation constants for NMP-SFRP and ATRP, proposed some simplified models, and carried out some calculations including thermal initiation and using a steady-state hypothesis (SSH) for radical concentrations. Krajnc et al. (2001) developed a semiempirical kinetic model for the INIFERTER controlled-radical homopolymerization of methyl methacrylate. Ward and Peppas (2000) have modeled gelation in free-radical INIFERTER copolymerization of vinyl/divinyl monomers, using the Percolation Theory.

It has been recognized that diffusion-controlled reactions are important in controlled-radical polymerization processes. As mentioned before, Shipp and Matyjaszewski (1999) and Butté et al. (1999) have used empirical models to take into account diffusion-controlled termination in their models for controlled-radical polymerization. Using electron-spin resonance (ESR) measurements, Yu et al. (2001) experimentally demonstrated that the deactivation of growing radicals in ATRP of poly(ethylene glycol) dimethacrylate was impeded by the restricted diffusion of the Cu(II)/ligand complex in polymer networks. The diffusion-controlled deactivation resulted in an increase in radical concentration, and the reaction was converted to a conventional free-radical polymerization process. Diffusion-controlled phenomena (autoacceleration and glass effects) in conventional free-radical polymerization have been studied and modeled for almost four decades, and have been reviewed elsewhere (Mita and Horie, 1987; Vivaldo-Lima et al., 1994; Gao and Penlidis, 1996; Dubé et al., 1997).

Although diffusion-controlled phenomena in controlled-radical polymerization have been addressed using fully empirical models (Shipp and Matyjaszewski, 1999; Butté et al., 2000), the abundant theoretical studies on the topic for conventional free-radical polymerization processes (e.g., Mita and Horie, 1987; Vivaldo-Lima et al., 1994; Gao and Penlidis, 1996; Dubé et al., 1997) provide a more mechanistic approach for modeling. In this article, diffusion-controlled reactions (radical termination, monomer propagation, and transfer between chains and catalyst in the forward and backward directions) are modeled using free-volume theory, and incorporating some important ideas and concepts in this area (Vivaldo-Lima et al., 1994). Experimental data of styrene, methyl methacrylate (MMA), and methyl acrylate (MA) homopolymerizations, in bulk and solution, are used to validate the diffusion-controlled kinetic model used in this article.

Model Development

Polymerization scheme

The elementary reactions considered to be the most important in ATRP, and the ones included in the kinetic model, are shown in Eq. 1:

$$\begin{array}{l} \qquad\qquad\quad k_p(+M) \\ \qquad\qquad\quad \uparrow\downarrow \quad k_{tr} \nearrow \quad RM_i \\ RM_iX + C \underset{k_b}{\overset{k_f}{\longleftrightarrow}} \quad RM_i^{\bullet} + XC \\ \qquad\qquad\quad \downarrow k_t(+RM_j^{\bullet}) \\ \qquad\qquad\quad RM_i + RM_j/RM_{i+j}R, \end{array} \tag{1}$$

where M, RX, C and XC are monomer, initiator, catalyst and oxidized catalyst; $RM_i^{\bullet}$, RM_iX, RM_i, and RM_iR are living chain, dormant chain, dead chain formed via termination by disproportionation and/or chain transfer, and dead chain formed via termination by combination; [ ], $[\ ]_0$ and subscript i denote molar concentration, initial molar concentration, and number of monomeric units in polymer chain; k is a rate constant with subscript f indicating forward, b, backward, p, propagation, t, termination (number average), td, termination by disproportionation, tc, termination by combination, and tr, transfer, respectively. $[M]_0$, $[RX]_0$, and $[C]_0$ are initial monomer, initiator, and catalyst concentrations, respectively.

For a batch reactor, the mass balances for living, dormant, and dead chains are given by Eqs. 2 to 9 (Zhu, 1999a). For a living chain,

$$\begin{aligned} \frac{d[RM_i^{\bullet}]}{dt} &= k_p[RM_{i-1}^{\bullet}][M] - k_p[RM_i^{\bullet}][M] \\ &\quad + k_f[RM_iX][C] - k_b[RM_i^{\bullet}][XC] - k_t[RQ_0^{\bullet}][RM_i^{\bullet}] \\ &\quad - k_{tr}[RM_i^{\bullet}], \end{aligned} \tag{2}$$

with $i = 0$

$$\begin{aligned} \frac{d[R^{\bullet}]}{dt} &= -k_p[R^{\bullet}][M] + k_f[RX][C] - k_b[R^{\bullet}][XC] \\ &\quad - k_t[RQ_0^{\bullet}][R^{\bullet}] - k_{tr}[R^{\bullet}]. \end{aligned} \tag{3}$$

For a dormant chain,

$$\frac{d[RM_iX]}{dt} = -k_f[RM_iX][C] + k_b[RM_i^{\bullet}][XC], \tag{4}$$

when $i = 0$

$$\frac{d[RX]}{dt} = -k_f[RX][C] + k_b[R^{\bullet}][XC]. \tag{5}$$

For a dead chain formed via radical termination by disproportionation and/or chain transfer to small molecules,

$$\frac{d[RM_i]}{dt} = k_{td}[RQ_0^\bullet][RM_i^\bullet] + k_{tr}[RM_i^\bullet] \quad (6)$$

$$\frac{d[R]}{dt} = k_{td}[RQ_0^\bullet][R^\bullet] + k_{tr}[R^\bullet]. \quad (7)$$

For a dead chain formed via radical termination by combination,

$$\frac{d[RM_iR]}{dt} = \frac{k_{tc}}{2}\sum_{j=0}^{i}[RM_j^\bullet][RM_{i-j}^\bullet] \quad (8)$$

$$\frac{d[RR]}{dt} = \frac{1}{2}k_{tc}[R^\bullet][R^\bullet]. \quad (9)$$

Method of moments

To follow molecular-weight development in terms of number and weight averages, the method of moments is used. The moments for radical, dormant, and dead polymer species are defined in Eq. 10:

$$[RQ_j^\bullet] = \sum_{i=0}^{\infty} i^j[RM_i^\bullet], \qquad [RQ_jX] = \sum_{i=0}^{\infty} i^j[RM_iX],$$

$$[RQ_j] = \sum_{i=0}^{\infty} i^j[RM_i], \qquad [RQ_jR] = \sum_{i=0}^{\infty} i^j[RM_iR]. \quad (10)$$

Upon application of the method of moments to Eqs. 2, 4, 6, and 8, Eqs. 11 to 14 are obtained for the jth moment of polymer radicals, dormant polymer species, dead polymer obtained by disproportionation termination, and dead polymer obtained by combination termination, respectively

$$\frac{d[RQ_j^\bullet]}{dt} = k_p\sum_{k=0}^{j-1}\binom{j}{k}[RQ_k^\bullet][M] + k_f[RQ_jX][C] - k_b[RQ_j^\bullet][XC] - k_t[RQ_0^\bullet][RQ_j^\bullet] - k_{tr}[RQ_j^\bullet] \quad (11)$$

$$\frac{d[RQ_jX]}{dt} = -k_f[RQ_jX][C] + k_b[RQ_j^\bullet][XC] \quad (12)$$

$$\frac{d[RQ_j]}{dt} = k_{td}[RQ_0^\bullet][RQ_j^\bullet] + k_{tr}[RQ_j^\bullet] \quad (13)$$

$$\frac{d[RQ_jR]}{dt} = \frac{k_{tc}}{2}\sum_{k=0}^{j}\binom{j}{k}[RQ_k^\bullet][RQ_{j-k}^\bullet]. \quad (14)$$

Setting $j = 0$ in Eqs. 11 to 14, Eqs. 15 to 18 for the moments of zeroth order are obtained

$$\frac{d[RQ_0^\bullet]}{dt} = k_f[RQ_0X][C] - k_b[RQ_0^\bullet][XC] - k_t[RQ_0^\bullet][RQ_0^\bullet] - k_{tr}[RQ_0^\bullet] \quad (15)$$

$$\frac{d[RQ_0X]}{dt} = -k_f[RQ_0X][C] + k_b[RQ_0^\bullet][XC] \quad (16)$$

$$\frac{d[RQ_0]}{dt} = k_{td}[RQ_0^\bullet][RQ_0^\bullet] + k_{tr}[RQ_0^\bullet] \quad (17)$$

$$\frac{d[RQ_0R]}{dt} = \frac{k_{tc}}{2}[RQ_0^\bullet][RQ_0^\bullet]. \quad (18)$$

When $j = 1$, the moment equations of first order are obtained.

$$\frac{d[RQ_1^\bullet]}{dt} = k_p[RQ_0^\bullet][M] + k_f[RQ_1X][C] - k_b[RQ_1^\bullet][XC] - k_t[RQ_0^\bullet][RQ_1^\bullet] - k_{tr}[RQ_1^\bullet] \quad (19)$$

$$\frac{d[RQ_1X]}{dt} = -k_f[RQ_1X][C] + k_b[RQ_1^\bullet][XC] \quad (20)$$

$$\frac{d[RQ_1]}{dt} = k_{td}[RQ_0^\bullet][RQ_1^\bullet] + k_{tr}[RQ_1^\bullet] \quad (21)$$

$$\frac{d[RQ_1R]}{dt} = k_{tc}[RQ_0^\bullet][RQ_1^\bullet]. \quad (22)$$

The second-order moment equations are given by Eqs. 23 to 26

$$\frac{d[RQ_2^\bullet]}{dt} = k_p[RQ_0^\bullet][M] + 2k_p[RQ_1^\bullet][M] + k_f[RQ_2X][C] - k_b[RQ_2^\bullet][XC] - k_t[RQ_0^\bullet][RQ_2^\bullet] - k_{tr}[RQ_2^\bullet] \quad (23)$$

$$\frac{d[RQ_2X]}{dt} = -k_f[RQ_2X][C] + k_b[RQ_2^\bullet][XC] \quad (24)$$

$$\frac{d[RQ_2]}{dt} = k_{td}[RQ_0^\bullet][RQ_2^\bullet] + k_{tr}[RQ_2^\bullet] \quad (25)$$

$$\frac{d[RQ_2R]}{dt} = k_{tc}[RQ_0^\bullet][RQ_2^\bullet] + k_{tc}[RQ_1^\bullet][RQ_1^\bullet]. \quad (26)$$

Since calculation of molecular-weight averages involves taking ratios of the overall moments for all polymer species of the same order, the overall moment equations for the total chain species can be established, and are given by Eqs. 27 to 30

$$\frac{d([RQ_0^\bullet] + [RQ_0X] + [RQ_0] + [RQ_0R])}{dt} = -\frac{k_{tc}}{2}[RQ_0^\bullet][RQ_0^\bullet] \quad (27)$$

$$\frac{d([RQ_1^\bullet] + [RQ_1X] + [RQ_1] + [RQ_1R])}{dt} = k_p[RQ_0^\bullet][M] \quad (28)$$

$$\frac{d([RQ_2^\bullet]+[RQ_2X]+[RQ_2]+[RQ_2R])}{dt} = k_p[RQ_0^\bullet][M] + 2k_p[RQ_1^\bullet][M] + k_{tc}[RQ_1^\bullet][RQ_1^\bullet] \quad (29)$$

$$\frac{d([RQ_j^\bullet]+[RQ_jX]+[RQ_j]+[RQ_jR])}{dt} = k_p \sum_{k=0}^{j-1} \binom{j}{k} [RQ_k^\bullet][M] + \frac{k_{tc}}{2} \sum_{k=1}^{j-1} \binom{j}{k} [RQ_k^\bullet][RQ_{j-k}^\bullet]. \quad (30)$$

The following conservation equations also apply, and can be used to simplify the material balances,

$$[RQ_0X]+[XC]=[RX]_0, \quad (31)$$

that is, the total number of atom X remains constant.

$$[C]+[XC]=[C]_0, \quad (32)$$

that is, the total number of catalyst C remains constant.

$$[RQ_0^\bullet]+[RQ_0X]+[RQ_0]+2[RQ_0R]=[RX]_0, \quad (33)$$

that is, the total number of initiator moiety R remains constant during polymerization.

$$[RQ_1^\bullet]+[RQ_1X]+[RQ_1]+[RQ_1R]=[M]_0-[M], \quad (34)$$

that is, the number of monomeric units remains constant.

The rate of monomer consumption is given by Eq. 35:

$$\frac{d[M]}{dt} = -k_p[RQ_0^\bullet][M]. \quad (35)$$

The number-average chain length can be calculated according to Eq. 36:

$$\bar{r}_n = \frac{[M]_0-[M]}{[RX]_0-[RX]-[R^\bullet]-[R]-[RR]-[RQ_0R]}. \quad (36)$$

In this work, only those molecules containing at least one monomeric unit ($i \geq 1$) are considered as polymer chains. The weight-average chain length can be calculated using Eq. 37:

$$\bar{r}_w = \frac{[RQ_2^\bullet]+[RQ_2X]+[RQ_2]+[RQ_2R]}{[M]_0-[M]}. \quad (37)$$

Finally, the polydispersity of the polymer molecular weight distribution can be calculated using Eq. 38

$$PD = \frac{\bar{r}_w}{\bar{r}_n}. \quad (38)$$

Diffusion-controlled reactions

Chain-length dependence of the kinetic constants is important when the reaction involves two large macromolecules, such as termination (whose kinetic rate constant is $k_t(n,m)$, where n and m are chain length of the reacting molecules). One simple way to account for the dependence of $k_t(n,m)$ on chain length is to use averages of $k_t(n,m)$ (Zhu and Hamielec, 1989; Vivaldo-Lima et al., 1994; Dubé et al., 1997).

In this article, diffusion-controlled reactions are modeled using equilibrium free-volume theory. Chain-length dependence of reactions among large macromolecules is considered here by using different averages of the kinetic rate constant for such reactions. In the mechanism shown in Eq. 1, only termination involves reaction between two large macromolecules. Propagation, transfer between growing chain and catalyst, and transfer to small molecules involve reaction between a large and a small molecule, and a single average of the corresponding kinetic rate constant is adequate in those cases.

A "series," rather than a "parallel" structure of the effective diffusion-controlled reactions, is used in this article. Equation 39 shows the structure of a "series" effective kinetic constant, and Eq. 40 corresponds to the "parallel" structure. In Eq. 39 $k_{\text{diff-attraction}}$ and $k_{\text{diff-separation}}$ refer to diffusional restrictions for attraction and separation of molecules, respectively. The classification of diffusion-controlled reactions as "series" or "parallel," and the demonstration that the "parallel" approach may be inadequate, were proposed and explained by Vivaldo-Lima et al. (1994). Only a few important ideas are discussed below.

$$k_{\text{eff}} = k_{\text{chem}} \frac{k_{\text{diff-attraction}}}{k_{\text{diff-separation}}} \quad (39)$$

$$\frac{1}{k_{\text{eff}}} = \frac{1}{k_{\text{chem}}} + \frac{1}{k_{\text{diff}}}. \quad (40)$$

On a first thought, the diffusional barriers for the attraction and separation of molecules might be considered the same. If that was the case, the ratio of these diffusion constants in Eq. 39 would be close to one. If the Smoluchowski equation is used to calculate the diffusion constants, the ratio of the diffusion constant for attraction to the diffusion constant for separation is given by Eq. 41

$$\frac{k_{\text{diff-attraction}}}{k_{\text{diff-separation}}} = \exp\left(-\frac{E_a-E_s}{RT}\right)\exp\left[-\left(\frac{\beta_a}{V_{fa}}-\frac{\beta_s}{V_{fs}}\right)\right]. \quad (41)$$

If it is assumed that the activation energy to overcome the attractive forces is the same for approach and separation of the molecules, namely, $E_a = E_s$, then the energy term in Eq. 41 will cancel out. An intuitively similar analysis would lead one to the conclusion that the free volume for attraction should be the same as the free volume for separation ($V_{fa} = V_{fs}$). However, the "overlap" factors (β_a and β_s) may not be the same. The overlap factor is related to the minimum hole size necessary for a diffusional jump; that is, the minimum volume of a hole that a molecule must find in its vicinity for thermal jumping (Fujita, 1993). The reason for the different values of the overlap factor for attraction and separation may

be related to the size of the molecules involved in these diffusion events. In the attraction event, the molecules are separated and their minimum hole volume is different from the one available for the larger molecule that results when they approach one another. The free-volume parameters that appear in Eqs. 42 to 48 are the difference between the overlap factors for attraction and separation, namely, $\beta = \beta_a - \beta_s$.

Bimolecular radical termination is modeled using number and weight averages of $k_t(n,m)$, as shown in Eqs. 42 and 43. The first term in both equations accounts for translational termination, and the other term in the equations refers to "reaction diffusion" or "residual" termination. Residual termination is calculated using Eq. 44. The number average of $k_t(n,m)$ is used to calculate polymerization rate, and number average chain length (to calculate all zero and first-order moments). The weight average is used to calculate weight-average chain length (second-order moments of radical, dormant, and dead polymer species). Subscript j in Eqs. 42 and 43 accounts for termination by combination, or termination by disproportionation; x in Eq. 43 is monomer conversion. The same value of β_t is assumed to be valid for both combination and disproportionation termination:

$$k_{tjn} = k_{tj}^0 \exp\left[-\beta_t\left(\frac{1}{v_f} - \frac{1}{v_{f_0}}\right)\right] + k_{tp}, \qquad j = c, d \quad (42)$$

$$k_{tjw} = k_{tjn}\left(\frac{\bar{r}_n}{\bar{r}_w}\right)^{x/2} + k_{tp}, \qquad j = c, d \quad (43)$$

$$k_{tp} = zk_p[M]. \quad (44)$$

The diffusion-controlled propagation kinetic rate constant is calculated using Eq. 45, which involves the reaction between a large macromolecule and a small monomer molecule

$$k_p = k_p^0 \exp\left[-\beta_p\left(\frac{1}{v_f} - \frac{1}{v_{f_0}}\right)\right]. \quad (45)$$

The reactions of reversible transfer between growing chains and catalyst, and the irreversible chain transfer to small molecules involve a large polymer molecule and a small molecule. Equations 46, 47, and 48 show the expressions used to calculate the activation, deactivation, and transfer to small-molecule reactions, respectively

$$k_f = k_f^0 \exp\left[-\beta_f\left(\frac{1}{v_f} - \frac{1}{v_{f_0}}\right)\right] \quad (46)$$

$$k_b = k_b^0 \exp\left[-\beta_b\left(\frac{1}{v_f} - \frac{1}{v_{f_0}}\right)\right] \quad (47)$$

$$k_{tr} = k_{tr}^0 \exp\left[-\beta_{tr}\left(\frac{1}{v_f} - \frac{1}{v_{f_0}}\right)\right]. \quad (48)$$

Fractional free-volume, v_f, is calculated using Eq. 49; v_{f_0} is fractional free-volume at initial conditions. The free-volume parameters, β_t, β_p, β_f, β_b, and β_{tr}, in Eqs. 42 and 45 to 48,

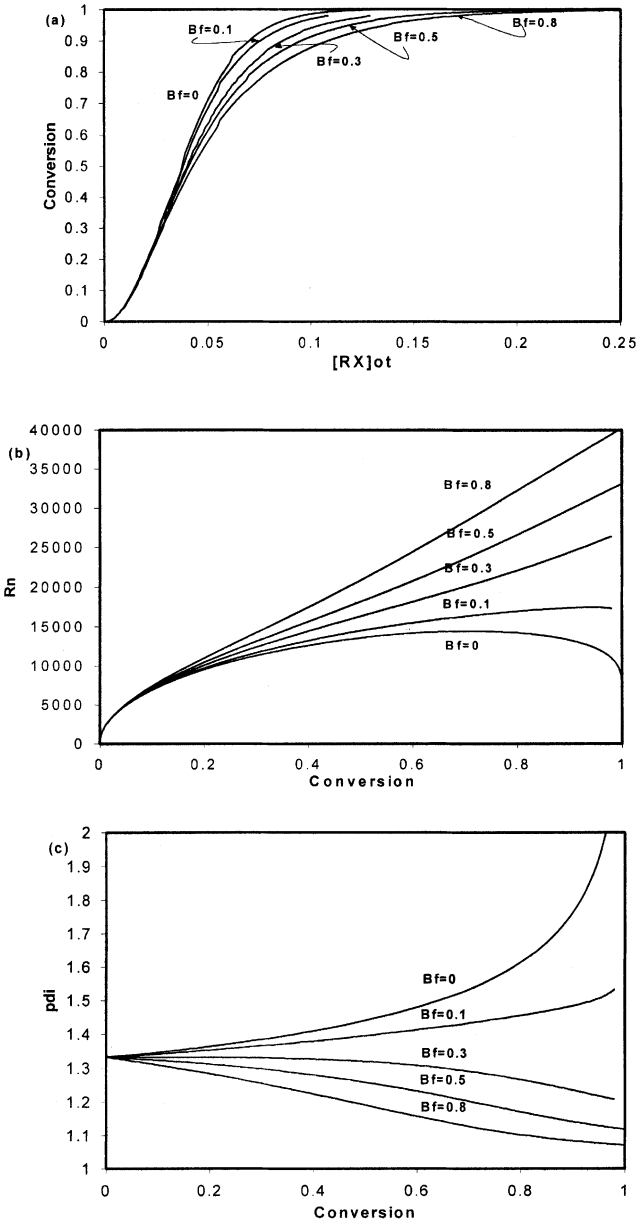

Figure 1. Effect of diffusion-controlled parameters of exchange reaction between dormant and active chains, β_b, and β_f, on (a) conversion, (b) number-average chain length, and (c) polydispersity, in ATRP.

$[M]_0/[RX]_0 = 1{,}000$; $[C]_0/[RX]_0 = 1$; $k_{f_0} = 1$ dm$^3\cdot$mol$^{-1}\cdot$s^{-1}; $k_{b_0} = 100$ dm$^3\cdot$mol$^{-1}\cdot$s^{-1}; $k_{p_0} = 1{,}000$ dm$^3\cdot$mol$^{-1}\cdot$s^{-1}; $k_{tr_0} = k_{t_0} = 0$ dm$^3\cdot$mol$^{-1}\cdot$s^{-1}; $z = 0$, $\beta_t = \beta_{tr} = \beta_p = 0$; and $\beta_b = \beta_f = 0$, 0.1, 0.3, 0.5, 0.8.

are "overlap" factors for the termination, propagation, activation, deactivation, and transfer reactions. These overlap factors account for the fact that the same free-volume is available to several molecules, and also for separation, once the molecules are in close proximity, yet have not reacted

$$v_f = \sum_{i=1}^{\#\text{ of components}} \left[0.025 + \alpha_i\left(T - T_{gi}\right)\right]\frac{V_i}{V_t}, \quad (49)$$

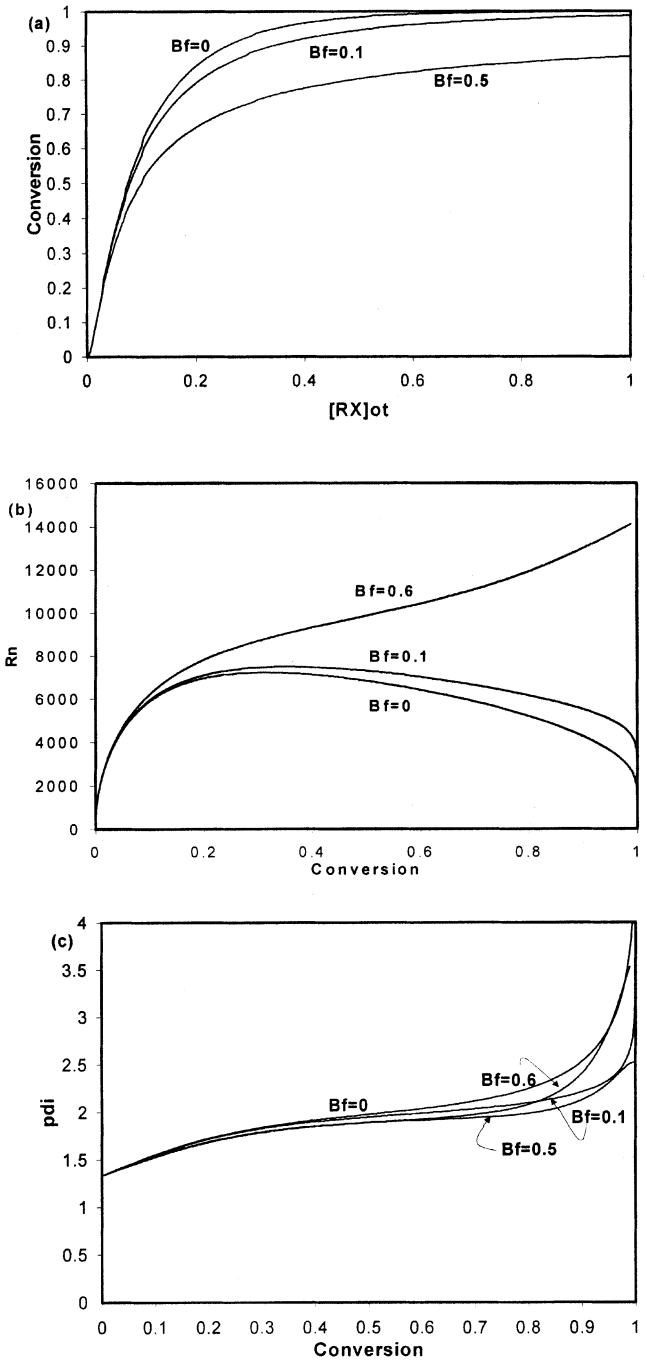

Figure 2. Effect of diffusion-controlled parameters of exchange reaction between dormant and active chains, β_b and β_f, on (a) conversion, (b) number-average chain length, and (c) polydispersity, in ATRP.

$[M]_0/[RX]_0 = 1{,}000$; $[C]_0/[RX]_0 = 1$; $k_{f_0} = 1$ dm^3·mol^{-1}·s^{-1}; $k_{b_0} = 1$ dm^3·mol^{-1}·s^{-1}; $k_{p_0} = 1{,}000$ dm^3·mol^{-1}·s^{-1}; $k_{td_0} = 10{,}000$ dm^3·mol^{-1}·s^{-1}; $k_{tr_0} = k_{tc_0} = 0$ dm^3·mol^{-1}·s^{-1}; $z = 0$; $\beta_t = \beta_{tr} = \beta_p = 0$; and $\beta_b = \beta_f = 0$, 0.1, 0.5, 0.8.

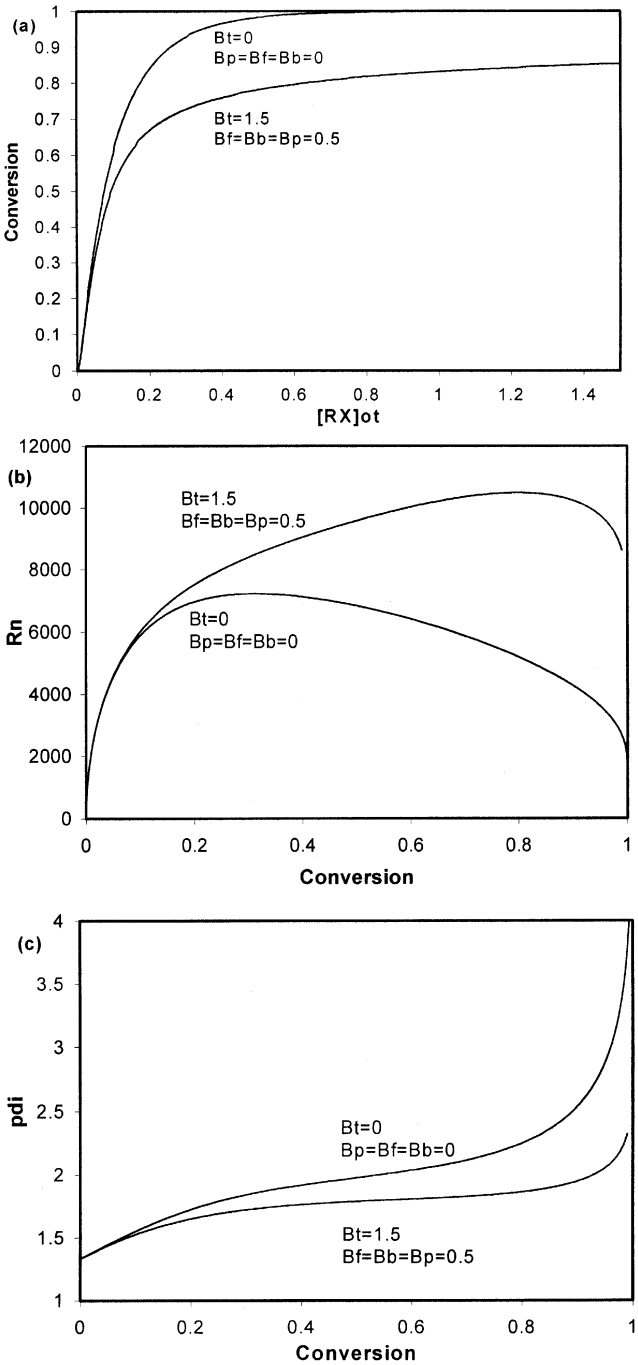

Figure 3. System with no diffusion-controlled effects ($\beta_p = \beta_b = \beta_f = \beta_{tr} = 0$, $\beta_t = 0$) vs. system with combined diffusion-controlled effects in termination, propagation, activation, and deactivation reactions ($\beta_p = \beta_b = \beta_f = 0.5$, $\beta_t = 1.5$, $\beta_{tr} = 0$), in ATRP.

Other parameters as in Figure 2.

where T and T_{gi} are reaction temperature and glass transition temperature of component i, respectively; α_i is the expansion coefficient for species i; and V_i and V_t are volume of species i and total system volume, respectively.

Results and Discussion

Qualitative simulation studies

A detailed simulation study on the qualitative effects of diffusion-controlled reactions on conversion, number-average

chain length, and polydispersity was carried out for this investigation, although only some of the main results are presented here. It was found that the effect of diffusion-controlled monomer propagation is to reduce polymerization rate, to decrease number-average chain length in a nonlinear fashion, and to significantly increase the polydispersity of the produced polymer. Radical termination is detrimental for the living character of a polymerization system. However, when termination is inevitable, the autoacceleration effect enhances the livingness of the system by reducing the value of the termination rate constant, k_t.

Figure 1 shows the combined effect of diffusion-controlled activation and deactivation reactions, when β_f is assumed equal to β_b. The system is living (termination and transfer to small molecules are absent). All other diffusion-controlled parameters in this figure are set equal to zero. The effect of simultaneously increasing the value of the diffusion-controlled parameter for activation and deactivation, is to reduce the polymerization rate, to increase the number-average chain length (providing a "more linear" profile), and decrease polydispersity. The case when termination by disproportionation is important, but no autoacceleration effect is present, is shown in Figure 2. It is observed that the presence of termination does not allow diffusion-controlled activation/deactivation to enhance the living behavior of the system as much as it was possible in a living radical system (Figure 1).

So far it has been noticed that diffusion-controlled termination enhances the livingness of the system (as compared with nondiffusion-controlled termination). Diffusion-controlled activation/deactivation also enhances the living behavior of the system, at least when $\beta_f = \beta_b$. On the other hand, it has been noticed that diffusion-controlled effects on propagation are detrimental to the living character of the reacting system. In order to qualitatively assess the performance of the system in a more real scenario, a simulation considering diffusion-controlled effects on propagation, termination, activation, and deactivation, was carried out. The results are shown in Figure 3. Overall, diffusion-controlled phenomena seem to favor the living behavior of the reacting system in ATRP. To generate Figure 3, typical values for the diffusion-controlled parameters were used.

It has been mentioned that the effect of diffusion-controlled activation/deactivation is to enhance the living character of the system. However, Yu et al. (2001) have experimentally observed that the deactivation of growing radicals in ATRP of poly(ethylene glycol) dimethacrylate was impeded by the restricted diffusion of the Cu(II)/ligand complex. They also observed an increase in radical concentration, which can be associated with diffusion-controlled termination, and an increase in polydispersity. They explained the transformation of the system from controlled to conventional free-radical polymerization in terms of the diffusion-controlled termination. These observations seem to contradict the predictions obtained with our model; that is, we predict diffusion-controlled termination and activation/deactivation to enhance the livingness of the system, while Yu et al. (2001) experimentally obtained the opposite. In order to address this apparent contradiction, it was decided to remove the hypothesis that $\beta_f = \beta_b$.

Figure 4 shows the effect of changing β_b, when β_f is fixed to 0.81 (solid lines labeled with values of $\beta_b = 0$, 0.1, 0.5, and 0.85). Also shown in Figure 4 is the effect of changing β_f when β_b is fixed to 0.85 (solid lines labeled with values of $\beta_f =$ 0, 0.1, 0.5, and 0.81). When β_b is increased, keeping β_f fixed, the polymerization rate is increased, the number average chain length is not significantly changed, but the polydispersity toward the end of the polymerization increases dramatically. A similar effect is obtained when β_f is increased, keeping β_b fixed, but the polymerization rate is increased much faster, and the magnitudes of the changes in number-average chain length and polydispersity differ. It is observed that diffusion-controlled effects are more severe in the activation reaction, although diffusion-controlled deactivation also reduces the livingness of the system, making it behave as conventional radical polymerization at moderately high conversions. These results demonstrate that the experimental observations of Yu et al. (2001) can be qualitatively reproduced with our model. Even though radical termination is theoretically responsible for the loss of livingness in a free-

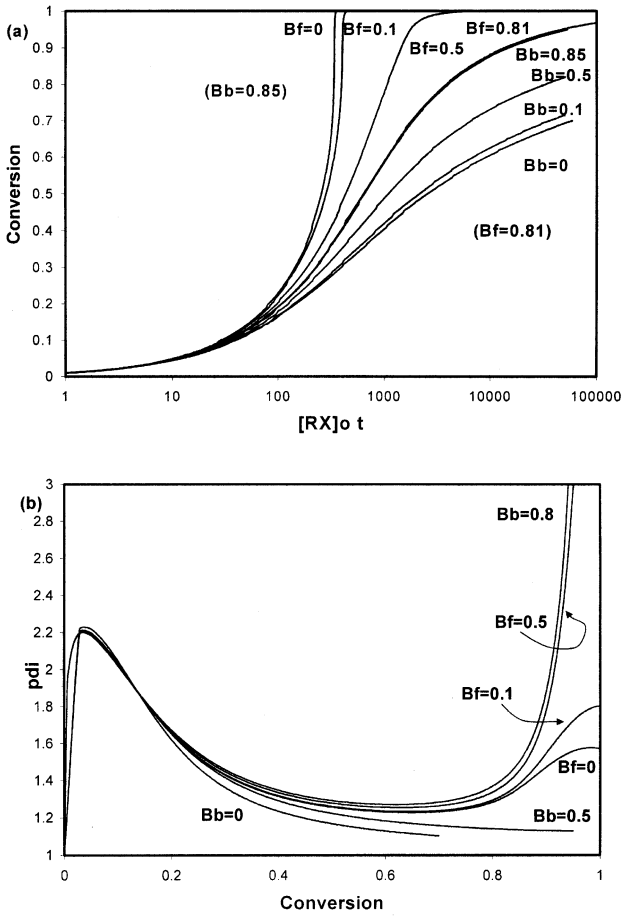

Figure 4. Effect of diffusion-controlled parameters of the exchange reactions between active and dormant species, k_b and k_f, on (a) conversion, and (b) polydispersity in ATRP of styrene at 383 K.

$[M]_0 = 8.7$ mol·dm^{-3}; $[C]_0/[RX]_0 = 1$; $[M]_0/[RX]_0 = 100$; $k_{p_0} = 1{,}609$ dm^3·mol^{-1}·s^{-1}; $k_{tc_0} = 4.98 \times 10^8$ dm^3·mol^{-1}·s^{-1}; $k_{f_0} = 0.042$ dm^3·mol^{-1}·s^{-1}; $k_{b_0} = 4.2 \times 10^5$ dm^3·mol^{-1}·s^{-1}; $k_{tr_0} = 0.13$ dm^3·mol^{-1}·s^{-1}; $k_{td_0} = 4.96 \times 10^{-11}$ dm^3·mol^{-1}·s^{-1}; $\beta_t = 1.71$; $\beta_p = 0.304$; and $\beta_{tr} = 0.5$. $\beta_f = 0.81$ in lines labeled as $\beta_b = 0$, 0.1, 0.5, 0.85; $\beta_b = 0.85$ in lines labeled as $\beta_f = 0$, 0.1, 0.5, 0.81.

Table 1. Parameters and Initial Conditions for Bulk ATRP of Styrene

Parameter	Value	Reference or Comments
k_p ($dm^3 \cdot mol^{-1} \cdot s^{-1}$)	1,600	Buback et al. (1995)
k_{tc_0}($dm^3 \cdot mol^{-1} \cdot s^{-1}$)	3.1304×10^8	Buback and Kuchta (1997)
k_{td_0} ($dm^3 \cdot mol^{-1} \cdot s^{-1}$)	4.9×10^{-11}	Vivaldo-Lima et al. (1994)
k_{tr_0} (s^{-1})	0.0	Neglected
k_{f_0} ($dm^3 \cdot mol^{-1} \cdot s^{-1}$)	0.45 (0.42)	Ohno et al. (1998); Goto and Fukuda (1999)
k_{b_0} ($dm^3 \cdot mol^{-1} \cdot s^{-1}$)	1.1×10^7	Ohno et al. (1998)
β_p (dimensionless)	0.3824 ± 0.0368	This work, EVM
β_t (dimensionless)	2.1255 ± 0.1905	This work, EVM
β_f (dimensionless)	0.4771 ± 0.0733	This work, EVM
β_b (dimensionless)	0.9727 ± 0.0953	This work, EVM
β_{tr} (dimensionless)	0.0	Neglected
z, ($dm^3 \cdot mol^{-1}$)	0 (135.0)	Vivaldo-Lima et al. (1994)
α_m, α_p, α_s (K^{-1})	0.001, 0.00048, 0.007(*)	Vivaldo-Lima et al. (1994)
T_{gm}, T_{gp}, T_{gs} (K)	185, 366.7, 123(*)	Vivaldo-Lima et al. (1994)
$[M]_0$ (mol dm^{-3}), styrene	8.7	Matyjaszewski et al. (1997)
$[RX]_0$ (mol dm^{-3}), 1-phenylethyl bromide (1-PEBr)	0.087	Matyjaszewski et al. (1997)
$[C]_0$ (mol dm^{-3}), CuBr/2(dNbipy)**	0.087	Matyjaszewski et al. (1997), $[C]_0 = [\text{CuBr}]_0 = [\text{dNbipy}]_0/2$
T (K)	383	Matyjaszewski et al. (1997)

**dNbipy = 4,4′-di-(5-nonyl)-2,2′-bipyridine.

radical polymerization, our simulations indicate that it is the diffusion-controlled activation (or deactivation), the one responsible for the large deviations from living behavior of the system, at high conversions.

Experimental validation of the model

In order to test the validity of the model, experimental data from the literature on styrene, methyl methacrylate, and methyl acrylate atom-transfer radical homopolymerizations, in bulk and solution, were used.

Batch and Solution ATRP of Styrene. For styrene ATRP, the experimental data of Matyjasweski et al. (1997) were used. Tables 1 and 2 summarize the values and the source of information for the kinetic rate constants, the initial conditions, the diffusion-controlled free-volume parameters, and other parameters used in the model.

To estimate the values of β_t, β_p, β_f, and β_b, the "errors-in-variables" method (EVM), which can be described as a weighed multivariable nonlinear regression procedure, was used. Conversion, number-average chain length, and weight-average chain length were used as responses. It is important to observe that the estimated values for β_f and β_b are different from each other, which appears to indicate that major deviations from the ideal controlled-radical behavior at high conversions may be due to the diffusion-controlled effects on the activation and deactivation reactions.

Table 2. Initial Conditions Used in Solution ATRP of Styrene

Parameter	Value	Reference or Comments
$[M]_0$ (mol·dm^{-3}), styrene	4.3	Matyjaszewski et al. (1997)
$[S]_0$ (mol·dm^{-3}), diphenyl ether	3.13	Matyjaszewski et al. (1997) (50% m^3/m^3)
$[RX]_0$ (mol dm^{-3}), 1-phenylethyl bromide (1-PEBr)	0.045	Matyjaszewski et al. (1997)
$[C]_0$ (mol·dm^{-3}), [CuBr]/2[dNbipy]	0.045	Matyjaszewski et al. (1997), $[C]_0 = [\text{CuBr}]_0 = [\text{dNbipy}]_0/2$
T (K)	383	Matyjaszewski et al. (1997)

Figure 5a shows experimental data (Matyjaszewski et al., 1997) (solid circles) and predicted profiles (closest solid line) of $\ln(M_0/M)$ vs. time for styrene ATRP, at 383 K. The triangles correspond to solution homopolymerization in diphenyl ether. The parameter estimation procedure was done with the experimental data for bulk ATRP. Therefore, the simulations for solution ATRP are true predictions, and provide an insight of the potential predictive power of the model. The agreement between experimental data and predicted profiles seems to be very good, except for the last experimental data point in the bulk case, which lies too far below the predicted profile. Since there are no repeats, and no experimental data are reported at higher conversions, it cannot be determined if the last experimental data point is in error, or if there is a model inconsistency at high conversions. In an attempt to explain that deviation, the nonzero value for parameter z of Eq. 44 was used. Equation 44 accounts for residual termination, which is important at high conversions. As shown in Figure 5a, for the lower of the two simulated profiles, the inclusion of z in the model improved the trend of the profile, but not significantly enough.

Figure 5b shows experimental data (solid circles) and the predicted profile (closest solid line) for number-average chain length vs. conversion. The agreement is quite good, except for the first data point in the low conversion zone. Figure 5c shows experimental data (solid circles) and the corresponding predicted profile for polydispersity vs. conversion. The agreement is very good. Since there are no experimental measurements in the high conversion range, it is not clear if the increase in polydispersity toward the end of the polymerization is that strong. According to our simulations (Figure 4), experimental data in the high conversion range are needed in order to obtain good estimates of β_f and β_b.

Figure 6 shows a plot of the different effective kinetic rate constants (k_{tn}, k_{tw}, k_p, k_f, and k_b) vs. conversion for bulk ATRP of styrene. Diffusion-controlled effects are more notorious on the radical termination and the radical/catalyst deactivation reactions. Since low polydispersity values were obtained, relative to conventional free-radical polymerization, the difference between k_{tn} and k_{tw} is not perceived in the plot. Propagation and activation decrease moderately, thus showing moderate diffusion-control effects. In the case of solution ATRP of styrene (not shown), all kinetic constants have a very slight value reduction with time, showing an almost constant behavior.

Solution ATRP of Methyl Methacrylate. To further test the performance of our diffusion-controlled ATRP (DC-ATRP) model, the experimental data of Wang et al. (1997) were used. Table 3 lists the values of all the parameters, physical properties, and initial conditions used to model this system. Although the conventional free-radical homopolymerization of methyl methacrylate has also been studied extensively, there were no experimentally determined values for the termination and activation (or deactivation) kinetic rate constants at the conditions of the reported experiments. Since there were no reported values for k_t measured experimentally, as was the case with styrene, the values obtained in a simulation study for cross-linking of MMA with ethylene glycol dimethacrylate (EGDMA) (Vivaldo-Lima et al., 2002) were used. Although the equilibrium constant for this ATRP system was measured experimentally and reported (Wang et al., 1997), neither of the individual values of k_f or k_b were reported. The 95% confidence intervals reported in Table 3 for MMA were values obtained in some of the EVM trials. The values in brackets show the ranges of variation that produced adequate results, combining all the EVM trials that produced reasonable values. Parameters marked with (*) in Tables 1 to 4 were not reported in the literature and were given reasonable values.

Figure 5 shows a comparison of experimental data (solid diamonds) and model predictions (closest profiles) for conversion (x), number-average chain length (n-CL), and polydispersity (PD). Overall the agreement is good, although the predicted $\ln(M_0/M)$ profile lies above the experimental data in the low-conversion regime, and below in the high-conversion regime. Once again, not having enough experimental data at the very low- and high-conversion regimes, and not having repeats, does not allow us to fairly judge the observed discrepancies in n-CL at PD in the low-conversion regime.

Although this polymerization was carried out in solution, Figure 7 shows that the activation and deactivation reactions are affected by diffusion-controlled phenomena, thus moderately reducing their kinetic rate constant values as polymerization proceeds. Propagation and termination do not show apparent diffusion-controlled effects at this polymerization conditions.

Bulk ATRP of Methyl Acrylate. The last experimental system considered in this article was the bulk ATRP of methyl acrylate. The experimental data used to compare with our model predictions were reported by Davis et al. (1999). Experimental initial conditions and model parameter values used to produce the predicted profiles for MA in Figure 5 are summarized in Table 4.

The parameter estimation stage for methyl acrylate was even more difficult than the preceding cases. There were no reliable, experimentally determined estimates available for k_p, k_t, k_f, and k_b. The range of variation for k_p and k_t in the literature was of orders of magnitude. The equilibrium constant, $K_{eq} = k_f/k_b$, was determined assuming that the k_p value was the same as the one for butyl acrylate polymerization (Davis et al., 1999). The values in brackets for k_p and k_b in Table 4 correspond to simulations that produced very similar profiles for n-CL and PD, and rather lower predictions (not shown in Figure 5) of x than the experimental data; that is, two quite different values of k_p could produce similar re-

Table 3. Initial Conditions and Parameters Used in Solution ATRP of Methyl Methacrylate

Parameter	Value	Reference or Comments
k_p ($dm^3 \cdot mol^{-1} \cdot s^{-1}$)	1,616	Gilbert et al. (1996)
k_{tc_0} ($dm^3 \cdot mol^{-1} \cdot s^{-1}$	1×10^7	Vivaldo-Lima et al. (2002) (see text)
k_{td_0} ($dm^3 \cdot mol^{-1} \cdot s^{-1}$)	9.21 x 10^7	Vivaldo-Lima et al. (2002) (see text)
k_{tr_0} (s^{-1})	0.046	set to an arbitrary low value
k_{f_0} ($dm^3 \cdot mol^{-1} \cdot s^{-1}$)	0.37 ± 0.041	EVM trials (see text)
k_{b_0} ($dm^3 \cdot mol^{-1} \cdot s^{-1}$)	5.286×10^5	$K_{eq} = k_f/k_b = 7 \times 10^{-7}$ (Wang et al., 1997)
β_p (dimensionless)	0.65 ± 0.32	This work, EVM
β_t (dimensionless)	6.64 ± 0.75 (4.0–7.0)	This work, EVM
β_f (dimensionless)	5.0 ± 0.023 (1.0–6.0)	This work, EVM
β_b (dimensionless)	3.0 ± 0.41 (2.5–5.5)	This work, EVM
β_{tr} (dimensionless)	0.5	Set to a typical value
z, ($dm^3 \cdot mol^{-1}$)	0 (135)	Vivaldo-Lima et al. (1994)
α_m, α_p, α_s (K^{-1})	0.001, 0.00048, 0.007(*)	Vivaldo-Lima et al. (2002)
T_{gm}, T_{gp}, T_{gs} (K)	167, 387, 170(*)	Vivaldo-Lima et al. (2002)
z, ($dm^3 \cdot mol^{-1}$)	0	
$[M]_0$ ($mol \cdot dm^{-3}$) MMA	4.67	Wang et al. (1997)
$[RX]_0$ ($mol \cdot dm^{-3}$), p-toluensulfonyl chloride	0.023	Wang et al. (1997)
$[C]_0$ ($mol \cdot dm^{-3}$), CuBr/2(dNbipy)	0.0115	Wang et al. (1997)
$[S]_0$ ($mol \cdot dm^{-3}$), diphenyl ether	3.1315	Wang et al. (1997) (50% m^3/m^3)
T(K)	363	Wang et al. (1997)

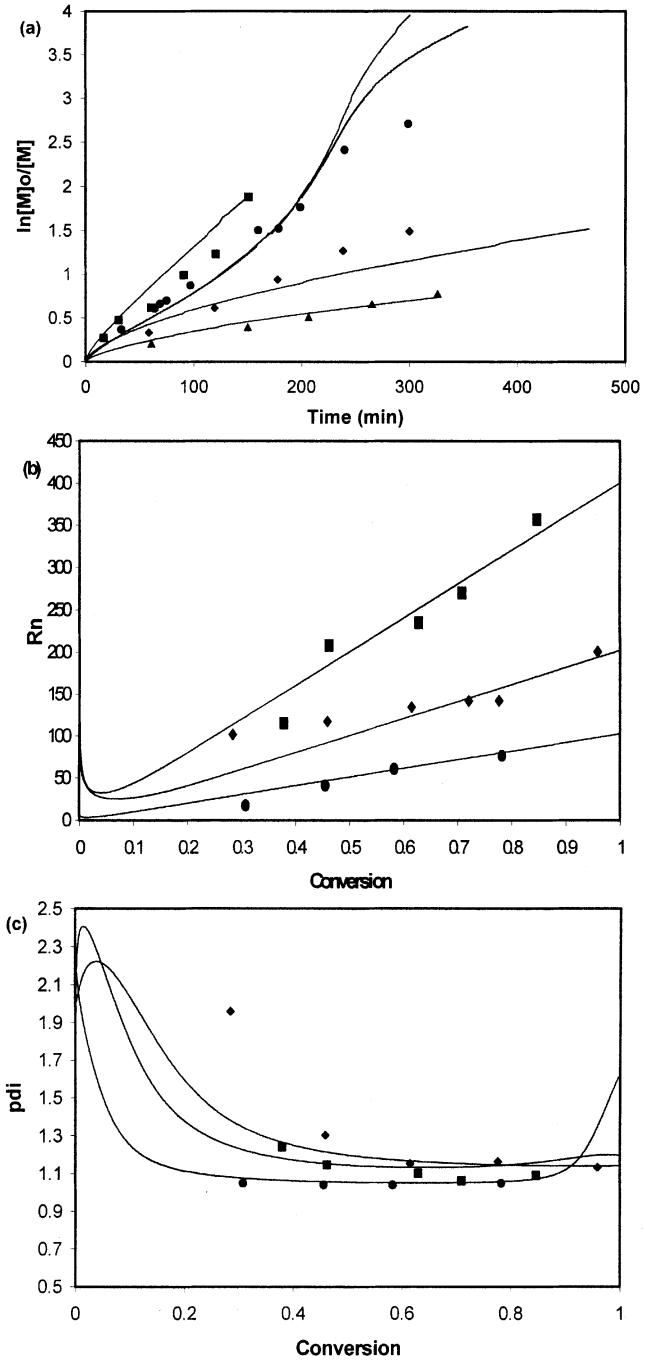

Figure 5. Model predictions vs. experimental data for bulk (●) and solution (▲) ATRP of styrene; solution ATRP of MMA (♦); and bulk ATRP of MA (■).

Polymerization conditions and kinetic parameters are shown in Tables 1, 2, 3, and 4, respectively. (a) $\ln([M]_0/[M])$ vs. time; (b) number average chain length vs. conversion; (c) polydispersity vs. conversion.

sults for x, n-CL, and PD. The agreement between experimental data and model predictions for x, n-CL, and PD, is reasonably good.

Figure 8 shows a plot of effective kinetic rate constants vs. conversion. It is observed that except for propagation, all the

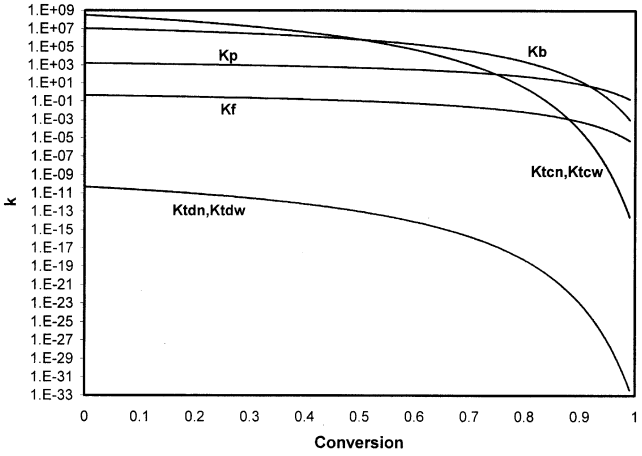

Figure 6. Model predictions of the evolution of k_{tn}, k_{tw}, k_p, k_f, and k_b in bulk ATRP of styrene, at conditions of Table 1.

reactions analyzed seem to be affected by diffusion constraints during the polymerization.

Evolution of Total Polymer Radical Concentration [RQ_0^*]. It is common practice in the modeling of polymerization processes to assume steady state in the concentration of polymer radicals. This is known as the "steady state hypothesis" (SSH). The SSH is reasonable for conventional free-radical polymerization processes, but its validity for controlled-radical polymerization processes cannot be assured without careful study. Some studies in controlled-radical polymerization have assumed the SSH to be valid in these processes (Fukuda et al., 2000). Since the kinetic model used in this article does not assume the steady state of the polymer radical concentration, and considering that very good agreement between experimental data and model predictions for styrene, methyl methacrylate, and methyl acrylate polymerizations was obtained, it was decided to analyze the evolution of [RQ_0^*] with

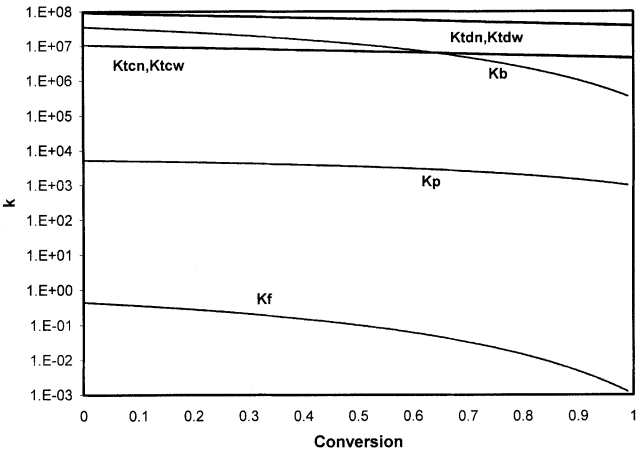

Figure 7. Model predictions of the evolution of k_{tn}, k_{tw}, k_p, k_f, and k_b in solution ATRP of methyl methacrylate, at conditions of Table 3.

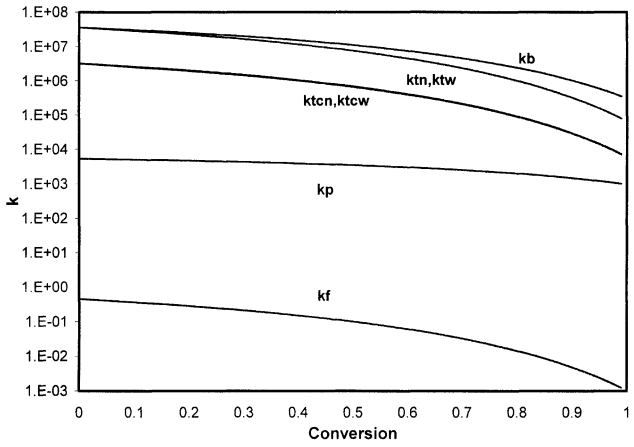

Figure 8. Model predictions of the evolution of k_{tn}, k_{tw}, k_p, k_f, and k_b in bulk ATRP of methyl acrylate, at conditions of Table 4.

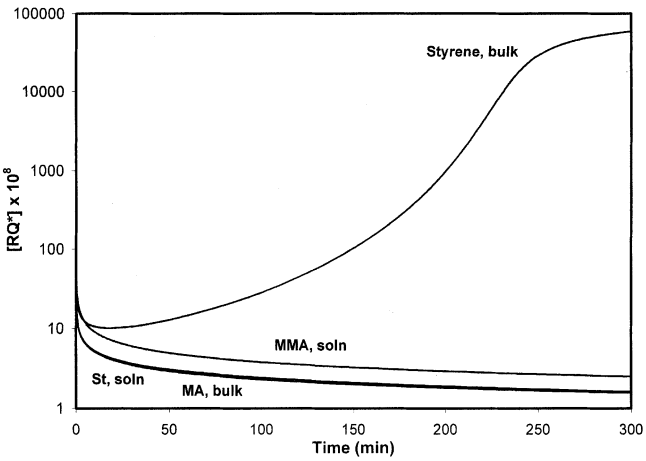

Figure 9. Model predictions of total polymer radical concentration vs. conversion for bulk and solution ATRP of styrene; solution ATRP of methyl methacrylate; and bulk ATRP of methyl acrylate.

At conditions of Tables 1, 2, 3, and 4, respectively.

time in order to get an insight into the validity of the SSH. Figure 9 shows the evolution of styrene, methyl methacrylate, and methyl acrylate polymerizations with time for the cases studied in this article, namely, styrene, methyl methacrylate, and methyl acrylate polymerizations. It is clearly observed that the SSH is not valid during the low and intermediate conversion range. Large variation in $[RQ_0^*]$ is observed during the first 150 min of reaction in the four cases shown in Figure 9.

Conclusions

Living radical polymerization processes such as ATRP are very sensitive to the values of the kinetic rate constants of the reactions involved in the mechanism, and in particular the value of the equilibrium constant of the activation/deactivation reactions. The present simulations show that diffusion-controlled effects are also fundamental in controlled-radical polymerization processes.

It has been shown that, if all reactions are present, diffusion-controlled (DC) propagation reduces the livingness of the system, DC termination enhances it, and DC activation/deactivation is a rather complex phenomenon. If the DC parameters for activation and deactivation are the same, it was found that the livingness of the system is enhanced, but if they are different, the livingness is reduced. The model presented here can explain the experimental observations of Yu

Table 4. Initial Conditions and Parameters Used in Bulk ATRP of Methyl Acrylate

Parameter	Value	Reference or Comments
k_p ($dm^3 \cdot mol^{-1} \cdot s^{-1}$)	5,333 (1,742)	Matheson et al. (1951) (see text)
k_{tc_0}($dm^3 \cdot mol^{-1} \cdot s^{-1}$)	3.254×10^6	Gao and Penlidis (1996); Matheson et al. (1951)
k_{td_0} ($dm^3 \cdot mol^{-1} \cdot s^{-1}$)	5.78×10^6	Gao and Penlidis (1996)
k_{tr_0} (s^{-1})	0.0	Neglected
k_{f_0} ($dm^3 \cdot mol^{-1} \cdot s^{-1}$)	0.45	Assumed equal to that of styrene
k_{b_0} ($dm^3 \cdot mol^{-1} \cdot s^{-1}$)	3.5714×10^7 (1.166×10^7)	Davis et al. (1999) (K_{eq} was adjusted, according to the k_p value for MA used in this article)
β_p (dimensionless)	0.1804 ± 0.0913 (0.2379 ± 0.042)	This work, EVM
β_t (dimensionless)	0.6633 ± 0.1528 (1.728 ± 0.33)	This work, EVM
β_f (dimensionless)	0.771 ± 0.129 (0.79 ± 0.143)	This work, EVM
β_b (dimensionless)	0.5	This work, EVM trials
β_{tr} (dimensionless)	0.0	Neglected
z, ($dm^3 \cdot mol^{-1}$)	0	
α_m, α_p, α_s (K^{-1})	0.001, 0.00048, 0.007(*)	Andrews and Grulke (1999)
T_{gm}, T_{gp}, T_{gs} (K)	185, 366.7, 423(*)	Andrews and Grulke (1999)
$[M]_0$ ($mol \cdot dm^{-3}$), methyl acrylate	11.2	Davis et al. (1999)
$[RX]_0$ ($mol \cdot dm^{-3}$), 2-bromopropionate	0.028	Davis et al. (1999)
$[C]_0$ ($mol \cdot dm^{-3}$), CuBr/2(dNbipy)	0.028	Davis et al. (1999)
T (K)	363	Davis et al. (1999)

et al. (2001) regarding observed DC deactivation in ATRP of EGDMA. The large deviation of their system from ideal living behavior at high conversions can be attributed to DC activation or DC deactivation.

The model presented in this article can reproduce very well the experimental data of x, n-CL, and PD, for bulk and solution ATRP of styrene, methyl methacrylate, and methyl acrylate. Reasonable good estimates of the kinetic and DC parameters of the model have been provided.

Finally, our simulations suggest that the SSH is inadequate in ATRP of styrene, methyl methacrylate, and methyl acrylate, at least in the low and intermediate conversion regimes, and in a temperature range between 363 and 383 K.

Acknowledgments

The authors wish to acknowledge financial support from the Science and Technology National Council (CONACYT) of Mexico, through Project 31170-U. One of the authors (O.D.-V.) acknowledges the undergraduate scholarship received from UNAM (PAPIIT Project IN120599), and the graduate (M. Eng.) scholarship granted to him by CONACYT.

Literature Cited

Andrews, R. J., and E. A. Grulke, "Solid State Properties, Glass Transition Temperatures of Polymers," *Polymer Handbook*, Chap. 6, J. Brandrup, E. H. Immergut, E. A. Grulke, A. Abe, and D. Bloch, eds., Wiley, New York (1999).

Buback, M., R. G. Gilbert, R. A. Hutchinson, B. Klumperman, F.-D. Kuchta, B. G. Manders, K. F. O'Driscoll, G. T. Russell, and J. Schweer, "Critically Evaluated Rate Coefficients for Free-Radical Polymerization. 1. Propagation Rate Coefficient for Styrene," *J. Macromol. Chem. Phys.*, **196**, 3267 (1995).

Buback, M., and F.-D. Kuchta, "Termination Kinetics of Free-Radical Polymerization of Styrene Over an Extended Temperature and Pressure Range," *Macromol. Chem. Phys.*, **198**, 1455 (1997).

Butté, A., G. Storti, and M. Morbidelli, "Kinetics of 'Living' Free Radical Polymerization," *Chem. Eng. Sci.*, **54**, 3225 (1999).

Colombani, D., "Chain-Growth Control in Free Radical Polymerization," *Prog. Poly. Sci.*, **22**, 1649 (1997).

Davis, K. A., H.-J. Paik, and K. Matyjaszewski, "Kinetic Investigation of the Atom Transfer Radical Polymerization of Methyl Acrylate," *Macromolecules*, **32**, 1767 (1999).

Dubé, M. A., J. B. P. Soares, A. Penlidis, and A. E. Hamielec, "Mathematical Modeling of Multicomponent Chain-Growth Polymerizations in Batch, Semibatch, and Continuous Reactors: A Review," *A, Ind. Eng. Chem. Res.*, **36**, 966 (1997).

Fujita, H., "Comments on Free Volume Theories for Polymer-Solvent Systems," *Chem. Eng. Sci.*, **48**, 3037 (1993).

Fukuda, T., A. Goto, and K. Ohno, "Mechanism and Kinetics of Living Radical Polymerizations," *Macromol. Rapid Commun.*, **21**, 151 (2000).

Gao, J., and A. Penlidis, "A Comprehensive Simulator/Database Package for Reviewing Free-Radical Homopolymerizations," *JMS-Rev. Macromol. Chem. Phys.*, **C36(2)**, 199 (1996).

Gilbert, R. G., "Critically-Evaluated Propagation Rate Coefficients in Free Radical Polymerizations. 1. Styrene and Methyl Methacrylate," *Pure Appl. Chem.*, **68**, 1491 (1996).

Goto, A., and T. Fukuda, "Determination of the Activation Rate Constants of Alkyl Halide Initiators for Atom Transfer Radical Polymerization," *Macromol. Rapid Commun.*, **20**, 633 (1999).

Greszta, D., and K. Matyjaszewski, "Mechanism of Controlled/'Living' Radical Polymerization of Styrene in the Presence of Nitroxyl Radicals. Kinetics and Simulations," *Macromolecules*, **29**, 7661 (1996).

Krajnc, M., I. Poljanšek, and J. Golob, "Kinetic Modeling of Methyl Methacrylate Free-Radical Polymerization Initiated by Tetraphenyl Biphosphine," *Polymer*, **42**, 4153 (2001).

Matheson, M. S., E. E. Auer, E. B. Bevilacgua, and E. J. Hart, "Rate Constants in Free Radical Polymerization. IV. Methyl Acrylate," *J. Amer. Chem. Soc.*, **73**, 5395 (1951).

Matyjaszewski, K., "Comparison and Classification of Controlled/Living Radical Polymerizations," *Controlled/Living Radical Polymerization*, K. Matyjaszewski, ed., ACS Symp. Ser. 768, Washington, DC, p. 2 (2000).

Matyjaszewski, K., T. E. Patten, and J. Xia, "Controlled/'Living' Radical Polymerization. Kinetics of the Homogeneous Atom Transfer Radical Polymerization of Styrene," *J. Amer. Chem. Soc.*, **119**, 674 (1997).

Mita, I., and K. Horie, "Diffusion-Controlled Reactions in Polymer Systems," *JMS-Rev. Macromol. Chem. Phys.*, **C27**(1), 91 (1987).

Ohno, K., A. Goto, T. Fukuda, J. Xia, and K. Matyjaszewski, "Kinetic Study on the Activation Process in an Atom Transfer Radical Polymerization," *Macromolecules*, **31**, 2699 (1998).

Otsu, T., and M. Yoshida, "Role of Initiator-Transfer Agent-Terminator (INIFERTER) in Radical Polymerizations—Polymer Design by Organic Disulfides as INIFERTERS," *Makromol. Chem. Rapid Commun.*, **3**, 127 (1982).

Shi, A.-C., M. K. Georges, and H. K. Mahabadi, "Kinetics of Controlled 'Living' Free Radical Polymerization: 1. Ideal Case," *Poly. React. Eng.*, **7**, 283 (1999).

Shipp, D. A., and K. Matyjaszewski, "Kinetic Analysis of Controlled/'Living' Radical Polymerizations by Simulations. 1. The Importance of Diffusion-Controlled Reactions," *Macromolecules*, **32**, 2948 (1999).

Shipp, D. A., and K. Matyjaszewski, "Kinetic Analysis of Controlled/'Living' Radical Polymerizations by Simulations. 2. Apparent External Orders of Reactants in Atom Transfer Radical Polymerization," *Macromolecules*, **33**, 1553 (2000).

Vivaldo-Lima, E., R. García-Pérez, and O. J. Celedón-Briones, "Modeling of the Free-Radical Copolymerization Kinetics with Crosslinking of Methyl Methacrylate/Ethylene Glycol Dimethacrylate Up to High Conversions and Considering Thermal Effects," *Rev. Soc. Quim. Mex.*, (2002).

Vivaldo-Lima, E., A. E. Hamielec, and P. E. Wood, "Auto-Acceleration Effect in Free-Radical Polymerization. A Comparison of the MH and CCS Models," *Poly. React. Eng.*, **2**(1&2), 16 (1994).

Wang, J.-L., T. Grimaud, and K. Matyjaszewski, "Kinetic Study of the Homogeneous Atom Transfer Radical Polymerization of Methyl Methacrylate," *Macromolecules*, **30**, 6507 (1997).

Ward, J. H., and N. A. Peppas, "Kinetic Gelation Modeling of Controlled Radical Polymerizations," *Macromolecules*, **33**, 5137 (2000).

Yu, Q., F. Zeng, and S. Zhu, "Atom Transfer Radical Polymerization of Poly(ethylene glycol) Dimethacrylate," *Macromolecules*, **34**, 1612 (2001).

Zhu, S., "Modeling of Molecular Weight Development in Atom Transfer Radical Polymerization," "Macromolecular Theory and Simulations," *Macromol. Theory Simulation*, **8**, 29 (1999a).

Zhu, S., "Modelling Stable Free Radical Polymerization," *J. Poly. Sci., Poly. Phys.*, **37**, 2692 (1999b).

Zhu, S., and A. E. Hamielec, "Chain-Length Dependent Termination for Free Radical Polymerization," *Macromolecules*, **22**, 3093 (1989).

Manuscript received June 22, 2001, and revision received Mar. 29, 2002.